



Chinese Journal of Structural Chemistry

结构化学(英文版)

ISSN 0254-5861, CN 35-1112/TQ

## 《Chinese Journal of Structural Chemistry》网络首发论文

题目: Influence of Doped Ions on Persistent Luminescence Materials: a Review  
作者: 张留伟, 沈瑞晨, 谈洁, 袁荃  
DOI: 10.14102/j.cnki.0254-5861.2011-3237  
收稿日期: 2021-04-26  
网络首发日期: 2021-07-21  
引用格式: 张留伟, 沈瑞晨, 谈洁, 袁荃. Influence of Doped Ions on Persistent Luminescence Materials: a Review . Chinese Journal of Structural Chemistry.  
<https://doi.org/10.14102/j.cnki.0254-5861.2011-3237>



**网络首发:** 在编辑部工作流程中, 稿件从录用到出版要经历录用定稿、排版定稿、整期汇编定稿等阶段。录用定稿指内容已经确定, 且通过同行评议、主编终审同意刊用的稿件。排版定稿指录用定稿按照期刊特定版式(包括网络呈现版式)排版后的稿件, 可暂不确定出版年、卷、期和页码。整期汇编定稿指出版年、卷、期、页码均已确定的印刷或数字出版的整期汇编稿件。录用定稿网络首发稿件内容必须符合《出版管理条例》和《期刊出版管理规定》的有关规定; 学术研究成果具有创新性、科学性和先进性, 符合编辑部对刊文的录用要求, 不存在学术不端行为及其他侵权行为; 稿件内容应基本符合国家有关书刊编辑、出版的技术标准, 正确使用和统一规范语言文字、符号、数字、外文字母、法定计量单位及地图标注等。为确保录用定稿网络首发的严肃性, 录用定稿一经发布, 不得修改论文题目、作者、机构名称和学术内容, 只可基于编辑规范进行少量文字的修改。

**出版确认:** 纸质期刊编辑部通过与《中国学术期刊(光盘版)》电子杂志社有限公司签约, 在《中国学术期刊(网络版)》出版传播平台上创办与纸质期刊内容一致的网络版, 以单篇或整期出版形式, 在印刷出版之前刊发论文的录用定稿、排版定稿、整期汇编定稿。因为《中国学术期刊(网络版)》是国家新闻出版广电总局批准的网络连续型出版物(ISSN 2096-4188, CN 11-6037/Z), 所以签约期刊的网络版上网络首发论文视为正式出版。

# Influence of Doped Ions on Persistent Luminescence Materials: a Review<sup>①</sup>

ZHANG Liu-Wei(张留伟) SHEN Rui-Chen(沈瑞晨)

TAN Jie<sup>②</sup>(谈洁) YUAN Quan<sup>②</sup>(袁荃)

*(Institute of Chemical Biology and Nanomedicine, State Key Laboratory of Chemo/Biosensing and Chemometrics, College of Chemistry and Chemical Engineering, Hunan University, Changsha 410082, China)*

**ABSTRACT** Persistent luminescence materials (PLMs) are potential luminescent materials which can remain emitting light after stopping the excitation. PLMs can avoid the autofluorescence of biological tissues, and play an important role in biosensing, targeted imaging and other fields. However, the applications of PLMs are often restricted by their weak persistent luminescence and short decay time after excitation. Doped ions will directly affect the luminescence centers and trap levels of PLMs, thereby leading to great differences in the optical performance of PLMs. Given this, the selection of doped ions to improve the optical performance of PLMs has become a fascinating research direction in recent years. At present, the published reviews mostly focus on the surface modifications and applications of PLMs. However, the influence of doped ions on the structure and optical performance of PLMs is seldom summarized. In this review, the influence of doped ions on the structure and optical performance of PLMs is introduced from three aspects: the type of doped ions, the number of types of doped ions, and the content of doped ions. Furthermore, we highlight recent achievements and mechanisms in the development of PLMs. Finally, we also propose and discuss the future opportunities and current challenges of ion-doped PLMs.

**Keywords:** persistent luminescence, doped ions, structure and optical performance;

**DOI:** 10.14102/j.cnki.0254-5861.2011-3237

## 1 INTRODUCTION

Persistent luminescence materials (PLMs) can absorb excitation energy and continue to emit light after the excitation is stopped<sup>[1-7]</sup>. In ancient China, natural minerals with luminous properties were made into luminous cups and night pearls. In 1866, Sidot et al. first prepared the sulfide PLMs ZnS:Cu<sup>2+</sup>, making PLMs enter the vision of researchers<sup>[8]</sup>. In 1968, Pailil et al. observed the persistent luminescence of SrAl<sub>2</sub>O<sub>4</sub>:Eu<sup>2+</sup>, pushing the researches of PLMs into a new stage<sup>[9, 10]</sup>. Subsequently, Matsuzawa et al. found that the phosphorescence intensity and phosphorescence time of SrAl<sub>2</sub>O<sub>4</sub>:Eu<sup>2+</sup>, Dy<sup>3+</sup> phosphors were more than ten times those of early PLMs<sup>[11]</sup>. Since then, many PLMs have been developed and widely used in transportation, military facilities, biosensing and other fields<sup>[12-15]</sup>.

The persistent luminescence inheritance makes PLMs proper candidates in material applications. Given this, many researchers

---

Received 26 April 2021; accepted 2 July 2021

① This research was supported by the Natural Science Foundation of Hunan Province, China (Nos. 2020JJ4173 and 2020JJ5038)

② Corresponding authors. Yuan Quan, professor, majoring in the synthesis of nanomaterials and related biological applications.

Tan Jie, associate professor, majoring in the design of chemically modified nucleic acids for biosensing. E-mails: yuanquan@whu.edu.cn and tanjie0416@hnu.edu.cn

are devoted to finding ways to improve the phosphorescence intensity and phosphorescence time of PLMs. The introduction of doped ions provides a possibility to improve the optical performance of PLMs<sup>[16-23]</sup>. For example, Yamamoto et al. discovered that the phosphorescence intensity and phosphorescence time of the materials were improved after introducing Dy<sup>3+</sup> ion into SrAl<sub>2</sub>O<sub>4</sub>:Eu<sup>2+</sup><sup>[11]</sup>. Liu et al. enhanced the phosphorescence intensity and prolonged the phosphorescence time exceeding 13 hours by adjusting the contents of Nd<sup>3+</sup> ion in Zn<sub>2</sub>Ga<sub>3-x-y</sub>Ge<sub>0.75</sub>O<sub>8</sub>:Cr<sub>x</sub>, Nd<sub>y</sub><sup>[24]</sup>. Studying the mechanisms of ion doping to enhance the optical performance of PLMs can help design PLMs with stronger phosphorescence intensity and longer phosphorescence time, thereby expanding the applications of PLMs.

Recently, reviews focus on synthesis methods, persistent luminescence mechanisms and applications of PLMs have been published. Li et al. systematically summarized the synthesis techniques, persistent luminescence mechanisms, characterizations and applications of PLMs<sup>[9]</sup>. Wang et al. summarized the persistent luminescence mechanisms, synthesis methods and biomedical applications of PLMs<sup>[25]</sup>. Singh et al. outlined the surface modifications, bioimaging applications of PLMs, and future research directions<sup>[26]</sup>. Doped ions play a vital role in improving the optical performance of PLMs. However, the influence of doped ions on the structure and optical performance of PLMs is seldom summarized. In this review, we mainly focus on how the optical performance of PLMs is affected by the type of doped ions, the number of types of doped ions, and the content of doped ions. Furthermore, the opportunities and challenges of PLMs in ion doping are also presented.

## 2 INFLUENCE OF DOPED IONS ON THE STRUCTURE AND OPTICAL PERFORMANCE OF PLMS

With the introduction of doped ions, different energy levels are produced in PLMs, resulting in different structures and optical performance. Herein, we classify and discuss how doped ions affect the structure and optical performance of PLMs based on the number of types of doped ions, the type of doped ions and the content of doped ions. To better demonstrate the influence of doped ions on PLMs, a summary of the main influence of doped ions on some common ion-doped PLMs is shown in Table 1.

**Table 1. Details of Host, Emitter, Co-dopants, Emission Region and Afterglow Decay of PLMs**

Host	Emitter	Co-dopants	Emission region	Afterglow decay	Ref.
SrAl <sub>2</sub> O <sub>4</sub>	Eu <sup>2+</sup>		450~700 nm	> 2 h	4
GdAlO <sub>3</sub>	Mn <sup>2+</sup>	Ge <sup>4+</sup>	600~840 nm	> 1200 s	64
Y <sub>3</sub> Al <sub>5-x</sub> Ga <sub>x</sub> O <sub>12</sub> (x = 0~4)	Ce <sup>3+</sup>	Bi <sup>3+</sup>	505 nm	54~68 min	67
ZnGa <sub>2</sub> O <sub>4</sub>	B <sup>3+</sup>		502,695 nm	600 s	18
Zn <sub>1.25</sub> Ga <sub>1.5</sub> Ge <sub>0.25</sub> O <sub>4</sub>	Cr <sup>3+</sup>	Yb <sup>3+</sup> , Er <sup>3+</sup>	650~850 nm	> 480 h	23
Li <sub>2</sub> ZnGeO <sub>4</sub>	Mn <sup>2+</sup>		550~800 nm	> 960 h	62
MgGeO <sub>3</sub>	Mn <sup>2+</sup>	Bi <sup>3+</sup>	680 nm	100 min	68
Y <sub>3</sub> Sc <sub>2</sub> Ga <sub>3</sub> O <sub>12</sub>	Ce <sup>3+</sup>		500 nm	100 min	69
CaMgSi <sub>2</sub> O <sub>6</sub>	Eu <sup>2+</sup>	Dy <sup>3+</sup> , Mn <sup>2+</sup>	468, 600, 670 nm	> 600s	66
Ca <sub>9</sub> Bi(PO <sub>4</sub> ) <sub>7</sub>	Ce <sup>3+</sup>	Tb <sup>3+</sup> , Mn <sup>2+</sup>	300~500 nm	5 h	70
Ca <sub>2</sub> BO <sub>3</sub> Cl	Eu <sup>2+</sup>	Dy <sup>3+</sup>	580 nm	48 h	71

Gd <sub>2</sub> O <sub>2</sub> S	Eu <sup>3+</sup>	Ti <sup>4+</sup> , Mg <sup>2+</sup>	580~720 nm	120 s	20
Lu <sub>2</sub> O <sub>3</sub>	Tb <sup>3+</sup>	Ca <sup>2+</sup>	543 nm	20~30 h	72
KY <sub>3</sub> F <sub>10</sub>	Tb <sup>3+</sup>		542 nm	108 s	73
AlN	Mn <sup>2+</sup>		570~700 nm	1 h	74

## 2.1 Influence of doped ions type on the structure and optical performance of PLMs

Due to the difference in the atomic structure and energy levels, various doped ions have different effects on the structure and optical performance of PLMs. Thus, the relationship between the type of doped ions and the structure and optical performance of PLMs is introduced in this section.

### 2.1.1 Cr<sup>3+</sup>-doped PLMs

Cr<sup>3+</sup> ion is usually introduced into PLMs to obtain red or near-infrared persistent luminescence resulting from its unique electronic transitions. Among them, Cr<sup>3+</sup>-doped ZnGa<sub>2</sub>O<sub>4</sub> is one of the research hotspots in PLMs. The ZnGa<sub>2</sub>O<sub>4</sub> crystal exhibits a cubic spinel structure, in which the Zn<sup>2+</sup> ion occupies the A-sites of the tetrahedron, and the Ga<sup>3+</sup> ion the B-sites of the octahedron<sup>[27, 28]</sup>. Cr<sup>3+</sup> ion tends to replace Ga<sup>3+</sup> ion in the distorted octahedral coordination for the reason that Cr<sup>3+</sup> ion has the same valence electron and ion radius as Ga<sup>3+</sup> ion, which makes the Cr<sup>3+</sup>-doped ZnGa<sub>2</sub>O<sub>4</sub> materials produce strong near-infrared phosphorescence at 696 nm<sup>[2, 29, 30]</sup>. Hao et al. found that the Cr<sup>3+</sup>-doped ZnGa<sub>2</sub>O<sub>4</sub> exhibits excellent optical performance, which can maintain phosphorescence for 10 hours after stopping the ultraviolet light irradiation<sup>[31]</sup>. Moreover, the author observed that the excitation spectrum of Cr<sup>3+</sup>-doped ZnGa<sub>2</sub>O<sub>4</sub> has three excitation bands of 250 ~ 350, 350 ~ 487, and 487 ~ 650 nm, which are caused by the host excitation band of ZnGa<sub>2</sub>O<sub>4</sub>, the charge transfer between ZnGa<sub>2</sub>O<sub>4</sub> and Cr<sup>3+</sup> ion, and the electronic transitions of Cr<sup>3+</sup> ion, respectively. Based on previous researches, Yan et al. further comprehensively studied the persistent luminescence mechanism of Zn<sub>2.94</sub>Ga<sub>1.96</sub>Ge<sub>2</sub>O<sub>10</sub>:Cr<sup>3+</sup><sup>[19]</sup>. As shown in Fig. 1, after the Zn<sub>2.94</sub>Ga<sub>1.96</sub>Ge<sub>2</sub>O<sub>10</sub> absorbs incident photons, the electrons of Zn<sub>2.94</sub>Ga<sub>1.96</sub>Ge<sub>2</sub>O<sub>10</sub> move to the conduction band and are trapped by native defects by means of nonradiative relaxation. When the ultraviolet light excitation is finished, the combination of holes and electrons released by native defects produces short phosphorescence. Since the absorption spectrum of Cr<sup>3+</sup> ion fully overlaps with the emission spectrum of Zn<sub>2.94</sub>Ga<sub>1.96</sub>Ge<sub>2</sub>O<sub>10</sub>, the energy absorbed by Zn<sub>2.94</sub>Ga<sub>1.96</sub>Ge<sub>2</sub>O<sub>10</sub> is transferred to Cr<sup>3+</sup> ion by means of nonradiative energy<sup>[32]</sup>. The continuous energy transfer causes the electrons of Cr<sup>3+</sup> ion to transform into three different excited states. Then, the electrons are trapped by the shallow electron traps or deep electron traps by means of nonradiative relaxation<sup>[33]</sup>. At the same time, the electron (*t*<sup>2</sup>*e*) fills the energy-matched traps in the form of <sup>4</sup>T<sub>1</sub> and <sup>4</sup>T<sub>2</sub> through the tunneling process. When the continuous energy transfer is stopped, the electron traps release the electrons which recombine with Cr<sup>3+</sup> ion, thereby producing a strong or ultra-long phosphorescence<sup>[19]</sup>.

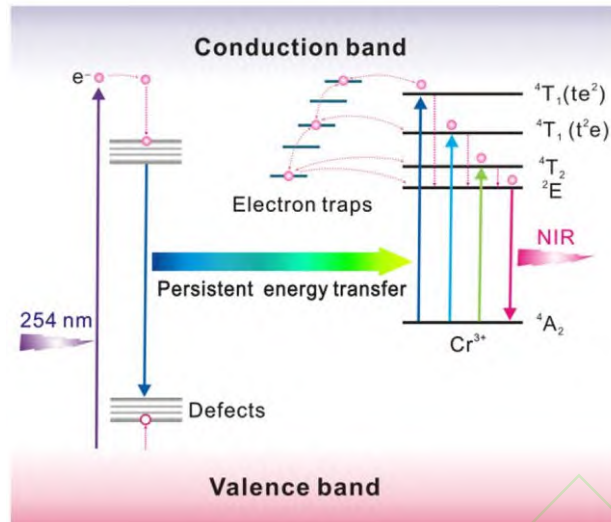


Fig. 1. Persistent energy transfer mechanism of Cr<sup>3+</sup>-doped ZnGa<sub>2</sub>O<sub>4</sub> materials

### 2. 1. 2 Mn<sup>2+</sup>-doped PLMs

Mn<sup>2+</sup> ion has a typical 3d<sup>5</sup> electronic configuration. The energy transitions of Mn<sup>2+</sup> ions are quite sensitive to the ligand/crystal field due to the participation of the *d* shell. Mn<sup>2+</sup> ions surrounded by anions can have different geometric structures, such as linear, octahedron, spherical, tetrahedron, or square plane. The environment of Mn<sup>2+</sup> ion at different crystal fields leads to different emission energy distributions and produces an emission band of 450 ~ 750 nm. For example, tetrahedral coordination of Mn<sup>2+</sup> ion produces green emission<sup>[34]</sup>, while octahedral coordination of Mn<sup>2+</sup> ion produces orange to red emission<sup>[35, 36]</sup>. Tan et al. researched the size, crystal structure and optical performance of Mn<sup>2+</sup>-doped ZnGa<sub>2</sub>O<sub>4</sub> with a typical rod-shaped structure in different environments<sup>[21]</sup>. The size of Mn<sup>2+</sup>-doped ZnGa<sub>2</sub>O<sub>4</sub> rapidly decreases as the pH increases from 6 to 7.5. In comparison, when the pH further increases to 9.5, the size of the Mn<sup>2+</sup>-doped ZnGa<sub>2</sub>O<sub>4</sub> materials slightly increases to 80 nm. The detailed crystal structure of the Mn<sup>2+</sup>-doped ZnGa<sub>2</sub>O<sub>4</sub> shows that the materials have lattice fringe (110) parallel to the direction of the crystal rod and lattice fringe (113) at an angle of 66 ° to the direction of the crystal rod<sup>[37]</sup>. Their interplanar spacing is 0.71 and 0.29 nm, indicating that the Mn<sup>2+</sup>-doped ZnGa<sub>2</sub>O<sub>4</sub> grows along the *c* axis<sup>[38]</sup>. The optical performance of ZnGa<sub>2</sub>O<sub>4</sub>:Mn<sup>2+</sup> materials was further researched by researchers<sup>[39]</sup>. The photoluminescence spectrum of Mn<sup>2+</sup>-doped ZnGa<sub>2</sub>O<sub>4</sub> materials shows that two emission peaks are detected at 450 and 480 nm, which are resulted from the native defects, for example, interstitial Zn and oxygen vacancies (Fig. 2a). When the pH is below 7.0, the intrinsic luminescence of the materials and the emission of Mn<sup>2+</sup> ions have a serious overlap. As the pH increases, the intrinsic luminescence intensity gradually decreases, and the emission band intensity of the Mn<sup>2+</sup> ion increases. The intrinsic luminescence almost disappears and is dominated by the green emission band of Mn<sup>2+</sup> when the pH increases to 9.5. In this case, the phosphorescence time of Mn<sup>2+</sup>-doped ZnGa<sub>2</sub>O<sub>4</sub> materials exhibits more than 100 s (Fig. 2b). According to the above results, a possible persistent luminescence mechanism of Mn<sup>2+</sup>-doped ZnGa<sub>2</sub>O<sub>4</sub> materials is proposed (Fig. 2c)<sup>[40, 41]</sup>. The excited electrons and holes produced under ultraviolet light excitation are trapped by electron traps and hole traps, respectively<sup>[42]</sup>. Then, some electrons get away from the electron traps under thermal stimulation and transfer to native defects, thereby resulting in the formation of emission peaks from ZnGa<sub>2</sub>O<sub>4</sub> materials<sup>[43]</sup>. The other part of the electrons escape and transfer to the excitation level of the Mn<sup>2+</sup> ion<sup>[44]</sup>. Subsequently, the recombination of holes and electrons

causes  $\text{Mn}^{2+}$  ion to emit green light<sup>[45]</sup>.

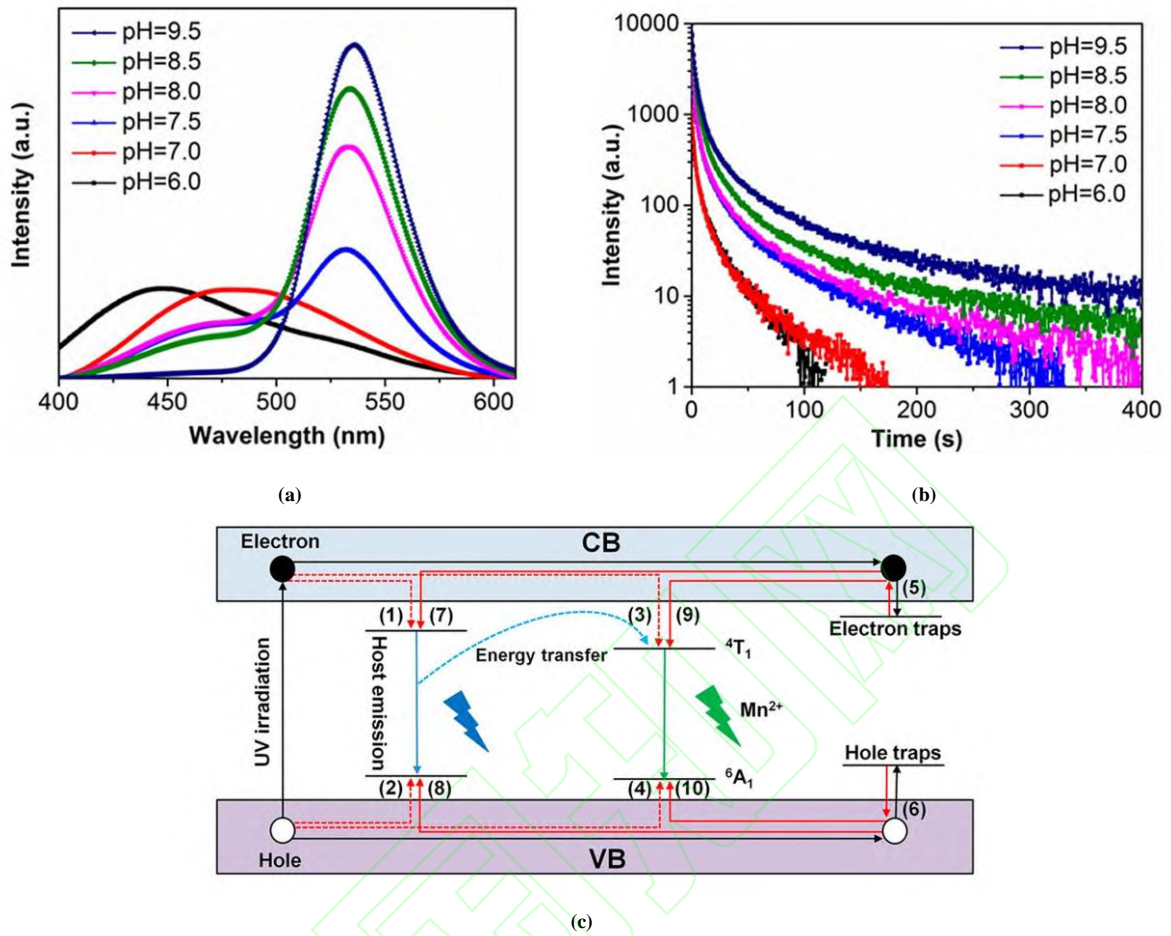


Fig. 2. (a) Photoluminescence spectrum, (b) phosphorescence decay curve, (c) persistent energy transfer mechanism of  $\text{ZnGa}_2\text{O}_4:\text{Mn}^{2+}$  materials

### 2. 1. 3 $\text{Eu}^{2+}$ -doped PLMs

$\text{Eu}^{2+}$  ion is a common doped ion in PLMs. The introduction of  $\text{Eu}^{2+}$  ion usually produces yellow, orange and red emissions for the reason that the crystal field reduces the emission energy of  $4f^65d^1$  electron configuration of  $\text{Eu}^{2+}$  ion<sup>[46]</sup>. Yang et al. researched the structure and optical performance of  $\text{Eu}^{2+}$ -doped  $\text{SrAl}_2\text{O}_4$  materials<sup>[4]</sup>. It is found that the crystal phase of the  $\text{Eu}^{2+}$ -doped  $\text{SrAl}_2\text{O}_4$  materials corresponds to the standard pattern, indicating that the structure of the  $\text{SrAl}_2\text{O}_4$  materials has not obviously changed after the introduction of  $\text{Eu}^{2+}$  ion. Moreover,  $\text{Eu}^{2+}$ -doped  $\text{SrAl}_2\text{O}_4$  shows a strong emission band of 450 ~ 700 nm and exhibits a phosphorescence time that exceeds 2 hours. Considering the structure and characteristics of  $\text{SrAl}_2\text{O}_4:\text{Eu}^{2+}$ , a possible persistent luminescence mechanism of  $\text{SrAl}_2\text{O}_4:\text{Eu}^{2+}$  is deduced. The  $\text{SrAl}_2\text{O}_4$  material as the host lattice absorbs the soft X-ray photon energy and stores it in electron traps. Then, the energy gets away from the electron traps and transfers to the  $4f^65d^1$  energy level in the  $\text{Eu}^{2+}$  ion, which causes the  $\text{Eu}^{2+}$  ion to produce radioactive transition luminescence.

### 2. 1. 4 $\text{B}^{3+}$ -doped PLMs

$\text{B}^{3+}$  ion can replace  $\text{Ga}^{3+}$  ion in  $\text{ZnGa}_2\text{O}_4$  materials to improve the optical performance of  $\text{ZnGa}_2\text{O}_4$  materials because of the

similarity of valence and chemical properties between  $\text{Ga}^{3+}$  and  $\text{B}^{3+}$  ions. Wang et al. researched the changes in the optical performance of  $\text{ZnGa}_2\text{O}_4$  materials after  $\text{B}^{3+}$ -doping<sup>[18]</sup>. Both  $\text{ZnGa}_2\text{O}_4$  and  $\text{ZnGa}_2\text{O}_4:\text{B}^{3+}$  can detect phosphorescence signal peaks at 502 and 695 nm. However, the phosphorescence decay curves indicate that the phosphorescence intensity and the phosphorescence time of  $\text{ZnGa}_2\text{O}_4:\text{B}^{3+}$  have been significantly improved compared with  $\text{ZnGa}_2\text{O}_4$ . According to previous reports, the proper trap depth is essential to achieve a better optical performance of PLMs<sup>[1, 47, 48]</sup>. There is a bold inference that the introduction of  $\text{B}^{3+}$  ion can also increase the content of electron traps  $\text{Ga}'_{\text{Zn}}$ , thus leading to the enhancement of optical performance of  $\text{ZnGa}_2\text{O}_4$  after  $\text{B}^{3+}$ -doping.

## 2.2 Influence of the number of types of doped ions on the structure and optical performance of PLMs

As above mentioned, the structure and optical performance of PLMs are closely related to the type of doped ions. Most PLMs used in practical applications need to be doped with multiple ions to enhance optical performance. The simultaneous introduction of multiple ions will affect not only the host of PLMs, but also the interaction among different ions. Therefore, we introduce the influence of the number of types of doped ions on the structure and optical performance of PLMs in this section.

### 2.2.1 $\text{Ge}^{4+}$ and $\text{Cr}^{3+}$ co-doped PLMs

The introduction of  $\text{Ge}^{4+}$  ion will change the width of the material bandgap due to its unique electronic structure. Thus, the change of structure and optical performance of  $\text{Ge}^{4+}$ ,  $\text{Cr}^{3+}$  co-doped PLMs is discussed<sup>[5]</sup>. Wang et al. found that the crystal phases of the  $\text{Cr}^{3+}$ -doped  $\text{ZnGa}_{1.995}\text{O}_4$  and  $\text{Ge}^{4+}$ ,  $\text{Cr}^{3+}$  co-doped  $\text{ZnGa}_{1.995}\text{O}_4$  materials are corresponding to the standard pattern, indicating that the structure of the materials has not obviously changed after  $\text{Ge}^{4+}$ ,  $\text{Cr}^{3+}$  co-doping. In addition, the emission spectra of  $\text{ZnGa}_{1.995}\text{O}_4:\text{Cr}^{3+}$  and  $\text{Zn}_{1.25}\text{Ga}_{1.5}\text{Ge}_{0.25}\text{O}_4:\text{Cr}^{3+}$  both present a near-infrared emission band of 650 ~ 900 nm<sup>[49, 50]</sup>. The phosphorescence decay curves show that the optical performance of  $\text{Zn}_{1.25}\text{Ga}_{1.5}\text{Ge}_{0.25}\text{O}_4:\text{Cr}^{3+}$  is better than that of  $\text{ZnGa}_{1.995}\text{O}_4:\text{Cr}^{3+}$ <sup>[5]</sup>. Based on the above results, the introduction of  $\text{Ge}^{4+}$  improves the filling efficiency of electron traps, thus increasing the phosphorescence time of the materials<sup>[23]</sup>.

### 2.2.2 $\text{Pr}^{3+}$ , $\text{Cr}^{3+}$ co-doped PLMs

The number and depth of the trap energy levels of PLMs are changed after the introduction of  $\text{Pr}^{3+}$  ion because of the special  $4f/5d$  electronic structure and abundant electronic transition types of  $\text{Pr}^{3+}$  ion. Therefore, the changes in structure and optical performance of  $\text{Zn}_{2.94}\text{Ga}_{1.96}\text{Ge}_2\text{O}_{10}$  after the introduction of  $\text{Pr}^{3+}$  and  $\text{Cr}^{3+}$  ions are discussed<sup>[19]</sup>. By analyzing the XRD pattern, the structure of  $\text{Zn}_{2.94}\text{Ga}_{1.96}\text{Ge}_2\text{O}_{10}:\text{Cr}^{3+}$ ,  $\text{Pr}^{3+}$  has not obviously changed, and the pure spinel phase is still maintained. Later, the author does in-depth studies on the optical performance of  $\text{Zn}_{2.94}\text{Ga}_{1.96}\text{Ge}_2\text{O}_{10}:\text{Pr}^{3+}$ ,  $\text{Cr}^{3+}$ . The electrons recombine with holes in the natural defects, thereby leading to a wide emission band of 350 ~ 660 nm. In addition, the  $\text{Cr}^{3+}$  ion provides a near-infrared emission band of 695 nm through the  ${}^2E \rightarrow {}^4A_2$  transition<sup>[27]</sup>, while the  $\text{Pr}^{3+}$  ion increases the phosphorescence time by adjusting the depth and density of traps based on the energy levels of  $4f$  electron configurations<sup>[51-55]</sup>. Similarly, Yu et al. did further research on the persistent luminescence mechanisms of  $\text{Zn}_3\text{Ga}_2\text{GeO}_8:\text{Cr}^{3+}$ ,  $\text{Pr}^{3+}$  to clarify the function of  $\text{Pr}^{3+}$  ion<sup>[56]</sup>. The introduction of  $\text{Pr}^{3+}$  ion deepens the trap energy level and increases the number of traps. Given this, a possible persistent luminescence mechanism of  $\text{Zn}_3\text{Ga}_2\text{GeO}_8:\text{Cr}^{3+}$ ,  $\text{Pr}^{3+}$  is proposed (Fig. 3). Trap A forms more traps than trap A' by introducing  $\text{Pr}^{3+}$  ion, thereby improving the phosphorescence intensity and the phosphorescence time of  $\text{Zn}_3\text{Ga}_2\text{GeO}_8:\text{Cr}^{3+}$ ,  $\text{Pr}^{3+}$  materials.

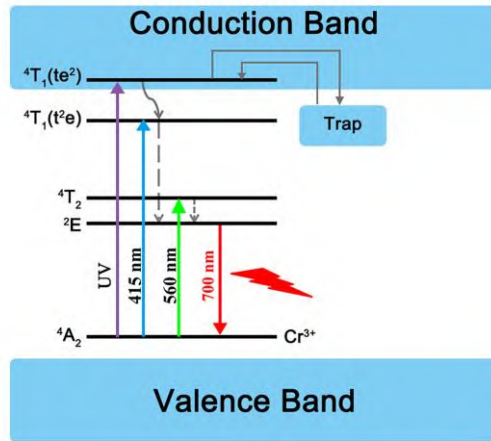
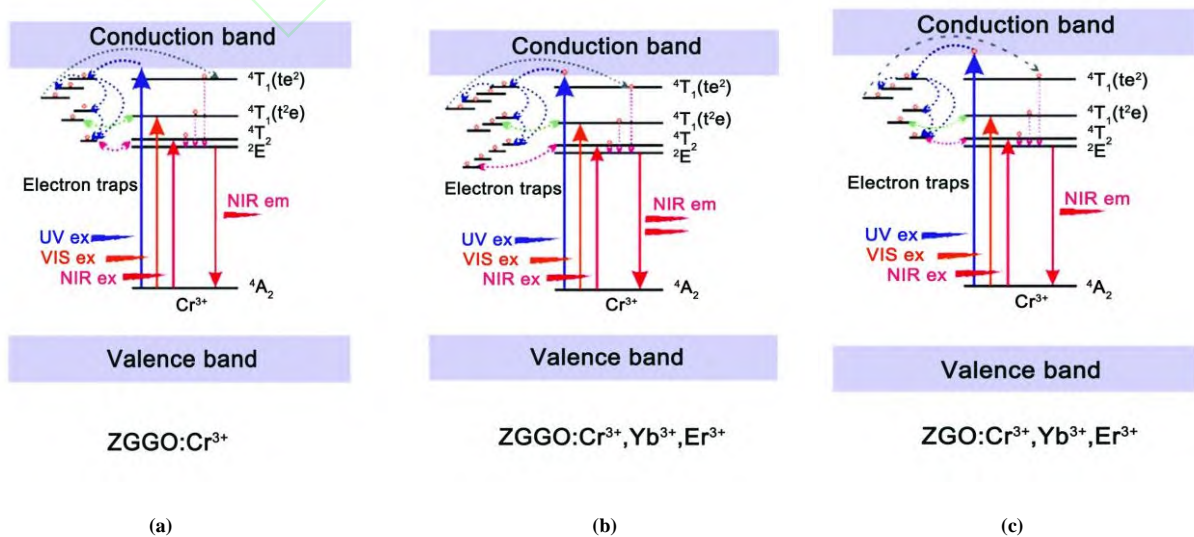


Fig. 3. Persistent luminescence mechanism of  $\text{Zn}_{2.94}\text{Ga}_{1.96}\text{Ge}_2\text{O}_{10}:\text{Pr}^{3+}, \text{Cr}^{3+}$  materials

### 2. 2. 3 $\text{Yb}^{3+}, \text{Er}^{3+}, \text{Cr}^{3+}$ co-doped PLMs

$\text{Yb}^{3+}$  ion and  $\text{Er}^{3+}$  ion are rare earth element ions used as luminescence centers, which are usually introduced into PLMs to change the density and depth of the trap levels resulting from their unique electronic structure. Consequently, the structure and optical performance of  $\text{Zn}_{1.25}\text{Ga}_{1.5}\text{Ge}_{0.25}\text{O}_4:\text{Yb}^{3+}, \text{Er}^{3+}, \text{Cr}^{3+}$  (ZGGO: $\text{Cr}^{3+}, \text{Yb}^{3+}, \text{Er}^{3+}$ ) with a pure spinel phase is discussed<sup>[23]</sup>. Yan et al. found that the structure of  $\text{Zn}_{1.25}\text{Ga}_{1.5}\text{Ge}_{0.25}\text{O}_4$  has not obviously changed after doping with  $\text{Yb}^{3+}, \text{Er}^{3+}$  and  $\text{Cr}^{3+}$  ion. Moreover, ZGGO: $\text{Cr}^{3+}, \text{Yb}^{3+}, \text{Er}^{3+}$  presents an excellent optical performance, and the phosphorescence time exceeds 20 days. Later, the author studied the persistent luminescence mechanism of ZGGO: $\text{Yb}^{3+}, \text{Er}^{3+}, \text{Cr}^{3+}$  (Fig. 4). The excited electrons are captured by electron traps under ultraviolet light irradiation, and then moves to deep traps by means of nonradiative relaxation. Subsequently, the combination of the excited electrons and the  $\text{Cr}^{3+}$  ion leads to the formation of a persistent phosphorescence signal after the ultraviolet radiation is stopped. The introduction of  $\text{Yb}^{3+}$  and  $\text{Er}^{3+}$  ions can not only provide the materials with additional electrons and energy levels, but also adjust the density and depth of traps<sup>[51, 57, 58]</sup>. The excited electrons are trapped in the deepest 4f energy levels of  $\text{Yb}^{3+}$  and  $\text{Er}^{3+}$  ions, thereby extending the time for the trapped electrons to return to the  ${}^2\text{E}$  energy level of  $\text{Cr}^{3+}$  ion (Fig. 4a, b)<sup>[58]</sup>, which also obviously prolongs the phosphorescence time of materials.





**Fig. 4. Persistent luminescence mechanism of (a) ZGGO:Cr<sup>3+</sup>, (b) ZGGO:Cr<sup>3+</sup>,Yb<sup>3+</sup>,Er<sup>3+</sup>, (c) ZGO:Cr<sup>3+</sup>,Yb<sup>3+</sup>,Er<sup>3+</sup>. ZGO refers to a zinc gallate matrix**

#### **2. 2. 4 Eu<sup>3+</sup>, Ti<sup>4+</sup> and Mg<sup>2+</sup> co-doped PLMs**

Viana et al. researched the structure and optical performance of Eu<sup>3+</sup>, Ti<sup>4+</sup>, Mg<sup>2+</sup> co-doped Gd<sub>2</sub>O<sub>2</sub>S materials with a pure hexagonal Gd<sub>2</sub>O<sub>2</sub>S phase<sup>[20]</sup>. The study found that Ti<sup>4+</sup> and Mg<sup>2+</sup> ions are trapping centers, and Eu<sup>3+</sup> ions are the emission centers. The Gd<sub>2</sub>O<sub>2</sub>S:Eu<sup>3+</sup>, Ti<sup>4+</sup>, Mg<sup>2+</sup> has an emission band of 580 ~ 720 nm due to the electronic transitions of Eu<sup>3+</sup> ion. Therefore, it can be inferred that the Eu<sup>3+</sup> ion plays the role of the luminescence center in the materials. Moreover, Gd<sub>2</sub>O<sub>2</sub>S: Eu<sup>3+</sup>, Ti<sup>4+</sup>, Mg<sup>2+</sup> has a longer phosphorescence time compared with Gd<sub>2</sub>O<sub>2</sub>S: Eu<sup>3+</sup> for the reason that Ti<sup>4+</sup> and Mg<sup>2+</sup> ions play an important in improving the density of trap energy levels. However, the particle size and crystal structure of Gd<sub>2</sub>O<sub>2</sub>S materials have not obviously changed after the introduction of Eu<sup>3+</sup>, Ti<sup>4+</sup> and Mg<sup>2+</sup> ions.

#### **2. 3 Influence of the content of doped ions on the structure and optical performance of PLMs**

As mentioned above, some doped ions play the role of the emission center of PLMs, while other doped ions will affect the number and depth of trap levels. Therefore, it is of great necessity to understand how the content of doped ions influences the structure and optical performance of PLMs. This section will discuss how the content of doped ions affects the structure and optical performance of PLMs.

##### **2. 3. 1 Pr<sup>3+</sup>, Cr<sup>3+</sup> co-doped PLMs**

Normally, Cr<sup>3+</sup> ion serves as the luminescence center of PLMs, while Pr<sup>3+</sup> ion affects the number and depth of trap levels. Yan et al. studied how the contents of Pr<sup>3+</sup> and Cr<sup>3+</sup> ions influence the structure and optical performance of PLMs. It is found that the increase of Cr<sup>3+</sup> content promotes the energy release of Zn<sub>2.94</sub>Ga<sub>1.96</sub>Ge<sub>2</sub>O<sub>10</sub>:Cr<sup>3+</sup>, Pr<sup>3+</sup>. Therefore, as the amount of Cr<sup>3+</sup> ion doping increases, the phosphorescence intensity and phosphorescence time of the material decrease<sup>[19, 27, 59]</sup>. Similarly, Zhang et al. studied the changes in particle size of Pr<sup>3+</sup>, Cr<sup>3+</sup> co-doped Zn<sub>2</sub>Ga<sub>2.98-x</sub>Ge<sub>0.75</sub>O<sub>8</sub> materials with different Pr<sup>3+</sup> contents<sup>[22]</sup>. It is found that the average size of the materials decreases with the increase of Pr<sup>3+</sup> contents. Considering that the doped ions can strongly affect the crystal growth rate through surface charge modification<sup>[60]</sup>, the size reduction of Zn<sub>2</sub>Ga<sub>2.98-x</sub>Ge<sub>0.75</sub>O<sub>8</sub>:Cr<sup>3+</sup>, Pr<sup>3+</sup> may be related to the influence of Pr<sup>3+</sup> ion on the surface charge of the material. Specifically, the surface charge distribution of the materials will be changed when the Pr<sup>3+</sup> ion is introduced into the materials, thereby reducing the growth rate. Subsequently, the optical performance of Pr<sup>3+</sup>, Cr<sup>3+</sup> co-doped Zn<sub>2</sub>Ga<sub>2.98-x</sub>Ge<sub>0.75</sub>O<sub>8</sub> materials is researched. As shown in Fig. 5a, the phosphorescence intensity and the phosphorescence time of the materials increase as the increase of Pr<sup>3+</sup> doping contents due to the changes in the trap levels of the materials caused by the introduction of Pr<sup>3+</sup> ion (Fig. 5b). When the content of Pr<sup>3+</sup> ion is too high, the luminescence performance will decrease due to the concentration quenching effect.

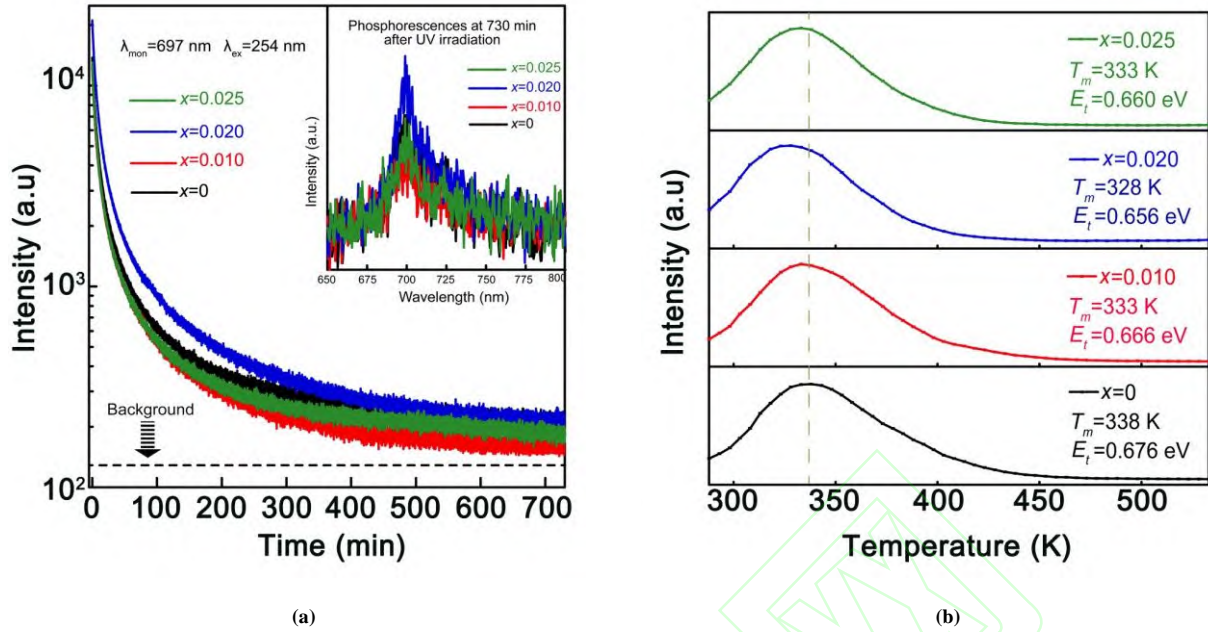


Fig. 5. (a) Phosphorescence decay curves of Pr<sup>3+</sup>, Cr<sup>3+</sup> co-doped Zn<sub>2</sub>Ga<sub>2.98-x</sub>Ge<sub>0.75</sub>O<sub>8</sub> materials with different Pr<sup>3+</sup> doping contents.

The inset presents the phosphorescence intensity of the materials after the ultraviolet light irradiation is stopped,

(b) Thermo-luminescence spectra of Pr<sup>3+</sup>, Cr<sup>3+</sup> co-doped Zn<sub>2</sub>Ga<sub>2.98-x</sub>Ge<sub>0.75</sub>O<sub>8</sub> materials with different Pr<sup>3+</sup> doping contents

### 2.3.2 Bi<sup>3+</sup>, Cr<sup>3+</sup> co-doped PLMs

Bi<sup>3+</sup> ion can significantly reduce the bandgap energy of PLMs and improve the efficiency of electron trap filling resulting from its unique 6s orbital. Tuerdi et al. researched the influence of crystalline structure, emission peak wavelength and phosphorescence time of ZnGa<sub>2</sub>O<sub>4</sub>:Bi<sup>3+</sup>, Cr<sup>3+</sup> materials with different Bi<sup>3+</sup> doping contents<sup>[16]</sup>. The Bi<sup>3+</sup> ion tends to replace Ga<sup>3+</sup> ion in ZnGa<sub>2</sub>O<sub>4</sub> with a similar ion radius, which makes the material produce higher periodic lattice distortion, thereby making the materials exhibit a longer phosphorescence time. When the doped ratio of Bi<sup>3+</sup> ion is low, the crystal phase of Cr<sup>3+</sup>, Bi<sup>3+</sup> co-doped ZnGa<sub>2</sub>O<sub>4</sub> materials corresponds to its standard spectrum, indicating that the structure of ZnGa<sub>2</sub>O<sub>4</sub> materials has not obviously changed after the introduction of Bi<sup>3+</sup> ion. However, when the doped ratio of Bi<sup>3+</sup> ion increases to 0.03, a strong peak related to the rhombohedral Bi<sup>3+</sup> structure at 28.01° is observed in the XRD pattern (Fig. 6a), illustrating that the original crystal structure of the materials is destroyed. Correspondingly, its optical performance is also reduced. The phosphorescence emission spectrum of ZnGa<sub>2</sub>O<sub>4</sub>:Bi<sup>3+</sup>, Cr<sup>3+</sup> materials with different Bi<sup>3+</sup> doping contents shows a red-shift of emission peak wavelength, which indicates that Bi<sup>3+</sup> ion reduces the crystal field intensity of the Cr<sup>3+</sup> ion (Fig. 6b).

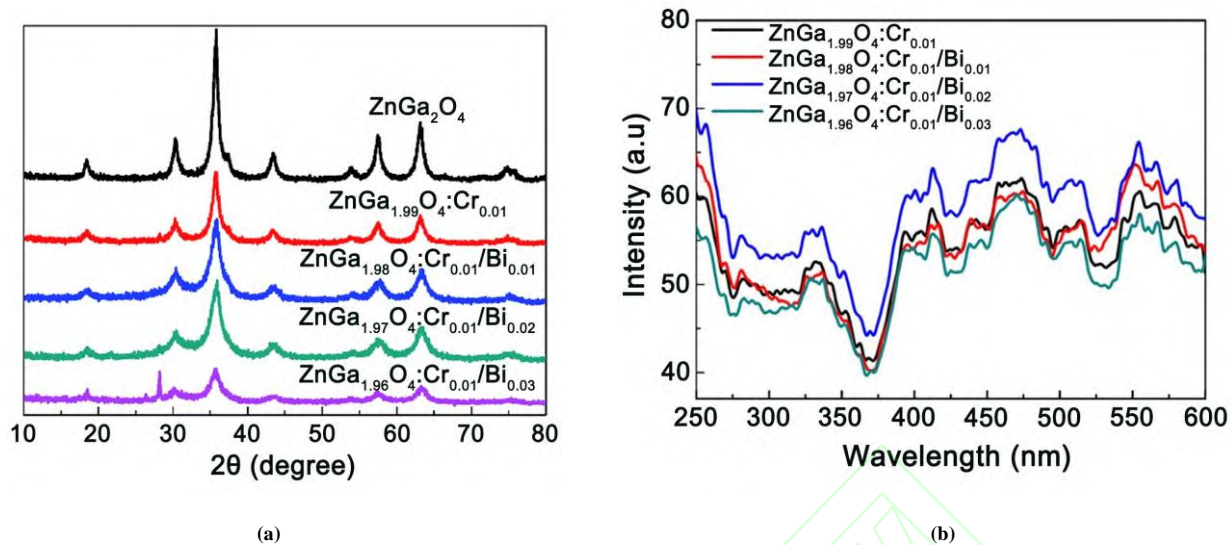


Fig. 6. (a) XRD patterns of  $\text{ZnGa}_2\text{O}_4$ ,  $\text{ZnGa}_2\text{O}_4:\text{Cr}^{3+}$  and  $\text{ZnGa}_2\text{O}_4:\text{Cr}^{3+}, \text{Bi}^{3+}$ ,  
 (b) Phosphorescence spectra of  $\text{ZnGa}_2\text{O}_4$ ,  $\text{ZnGa}_2\text{O}_4:\text{Cr}^{3+}$  and  $\text{ZnGa}_2\text{O}_4:\text{Cr}^{3+}, \text{Bi}^{3+}$

### 2. 3. 3 $\text{B}^{3+}$ , $\text{Cr}^{3+}$ co-doped PLMs

As mentioned above, the introduction of  $\text{B}^{3+}$  ion can improve the optical performance of  $\text{ZnGa}_2\text{O}_4$ . On this basis, the researchers studied the influence of doped ion content on PLMs. For example, Yan et al. synthesized  $\text{ZnGa}_2\text{O}_4:\text{B}^{3+}, \text{Cr}^{3+}$  materials by hydrothermal method, and studied the optical performance of  $\text{ZnGa}_2\text{O}_4:\text{Cr}^{3+}$  with different  $\text{B}^{3+}$  doping contents<sup>[17]</sup>. The XRD pattern presents that the structure of the material has not obviously changed after doping with the  $\text{B}^{3+}$  and  $\text{Cr}^{3+}$  ions. Besides, the emission wavelength of the materials has not obviously changed when the  $\text{B}^{3+}$  ion is introduced into the materials, which indicates that the  $\text{B}^{3+}$  ion does not play the role of luminescence center in the materials. At the same time, the improvement of the optical performance of materials shows that the introduction of  $\text{B}^{3+}$  ion injects new electron traps into the materials and increases the content of electron traps.

### 2. 3. 4 $\text{Eu}^{3+}$ , $\text{Ti}^{4+}$ and $\text{Mg}^{2+}$ co-doped PLMs

$\text{Eu}^{3+}$ ,  $\text{Ti}^{4+}$  and  $\text{Mg}^{2+}$  ions will act as luminescence centers or trap levels to affect the optical performance of the material. Therefore, studying the optical performance of  $\text{Gd}_2\text{O}_2\text{S}:\text{Eu}^{3+}, \text{Ti}^{4+}$  and  $\text{Mg}^{2+}$  materials with different doping contents will help us better understand the role of these ions in the material<sup>[20]</sup>. The study found that  $\text{Eu}^{3+}$  ion provides trap levels for electron-hole recombination, and  $\text{Ti}^{4+}$  ion provides electron traps to achieve the formation of the phosphorescence signal. Since  $\text{Ti}^{4+}$  ion replaces  $\text{Gd}^{3+}$  ion and destroys the charge conservation of the materials, it is necessary to introduce  $\text{Mg}^{2+}$  ion to maintain charge balance. In addition, as the doping contents of  $\text{Mg}^{2+}$  ion increase, the phosphorescence intensity of the material increases. This indicates that the introduction of  $\text{Mg}^{2+}$  ion can induce the formation of intermediate trap levels in the material, which prolongs the storage time of the carriers in the material, thus realizing the improvement of the persistent performance of the materials<sup>[61]</sup>.

Apart from the ion-doped PLMs mentioned above, other doped ions also have an impact on the structure and optical performance. For example,  $\text{Li}_2\text{ZnGeO}_4:\text{Mn}^{2+}$ <sup>[62]</sup>,  $\text{SrAl}_2\text{O}_4:\text{Eu}^{2+}$ ,  $\text{Dy}^{3+}$ <sup>[63]</sup>,  $\text{GdAlO}_3:\text{Mn}^{4+}$ ,  $\text{Ge}^{4+}$ <sup>[64]</sup>,  $\text{LaAlO}_3:\text{Mn}^{4+}$ ,  $\text{Ge}^{4+}$ <sup>[65]</sup>,  $\text{CaMgSi}_2\text{O}_6:\text{Eu}^{2+}$ ,  $\text{Dy}^{3+}$ ,  $\text{Mn}^{2+}$ <sup>[66]</sup>,  $\text{Y}_3\text{Al}_{5-x}\text{Ga}_x\text{O}_{12}:\text{Ce}^{3+}, \text{Bi}^{3+}$  ( $x = 0 \sim 4$ )<sup>[67]</sup>,  $\text{MgGeO}_3:\text{Mn}^{2+}, \text{Bi}^{3+}$ <sup>[68]</sup>,  $\text{Y}_3\text{Sc}_2\text{Ga}_3\text{O}_{12}:\text{Ce}^{3+}$ <sup>[69]</sup>,

Ca<sub>9</sub>Bi(PO<sub>4</sub>)<sub>7</sub>:Ce<sup>3+</sup>, Tb<sup>3+</sup>, Mn<sup>2+</sup>[70], Ca<sub>2</sub>BO<sub>3</sub>Cl:Eu<sup>2+</sup>, Dy<sup>3+</sup>[71], Lu<sub>2</sub>O<sub>3</sub>:Tb<sup>3+</sup>, Ca<sup>2+</sup>[72], KY<sub>3</sub>F<sub>10</sub>:Tb<sup>3+</sup>[73] and AlN:Mn<sup>2+</sup>[74].

### 3 CONCLUSION

In this review, we mainly focus on the impact of the type of doped ions, the number of types of doped ions, and the content of doped ions on the structure and optical performance of PLMs. In the past decade, although various doped ions have been widely used to improve the optical performance of PLMs, there is still much work to do in the future. First, in the actual preparation process, the optical performance of PLMs will be affected by the symmetry of matrix lattice, the radius of activated ions, and the electronegativity and distribution of external electron cloud. This should be paid more attention to by researchers. Second, exploring the relationship between doped ions and the host lattice and investigating the influence of the defects caused by doped ions on the storage time of the carriers. At present, these issues still have no exact quantitative relationship, and further researches are needed. Third, understanding the role of trap types, trap contents and probability of trapping electrons in the researches of the persistent luminescence mechanisms. Forth, exploring new doped ions and substrates. For example, most current PLMs are based on aluminates, gallates and silicates matrices. It is necessary to find new matrices with excellent properties. Collectively, with the deepening research of PLMs, ion-doped PLMs with higher luminescence intensity and phosphorescence lifetime will have a broad development prospect.

### REFERENCES

- (1) Van den Eeckhout, K.; Smet, P. F.; Poelman, D. Persistent luminescence in Eu<sup>2+</sup>-doped compounds: a review. *Materials* **2010**, *3*, 2536–2566.
- (2) Zhou, Z.; Zheng, W.; Kong, J.; Liu, Y.; Huang, P.; Zhou, S.; Chen, Z.; Shi, J.; Chen, X. Rechargeable and LED-activated ZnGa<sub>2</sub>O<sub>4</sub>:Cr<sup>3+</sup> near-infrared persistent luminescence nanoprobes for background-free biodetection. *Nanoscale* **2017**, *9*, 6846–6853.
- (3) Song, L.; Li, P. P.; Yang, W.; Lin, X. H.; Liang, H.; Chen, X. F.; Liu, G.; Li, J.; Yang, H. H. Low-dose X-ray activation of W(VI)-doped persistent luminescence nanoparticles for deep-tissue photodynamic therapy. *Adv. Funct. Mater.* **2018**, *28*, 1707496–10.
- (4) Song, L.; Lin, X. H.; Song, X. R.; Chen, S.; Chen, X. F.; Li, J.; Yang, H. H. Repeatable deep-tissue activation of persistent luminescent nanoparticles by soft X-ray for high sensitivity long-term in vivo bioimaging. *Nanoscale* **2017**, *9*, 2718–2722.
- (5) Liu, Y.; Liu, J. M.; Zhang, D.; Ge, K.; Wang, P.; Liu, H.; Fang, G.; Wang, S. Persistent luminescence nanophosphor involved near-infrared optical bioimaging for investigation of foodborne probiotics biodistribution in vivo: a proof-of-concept study. *J. Agric. Food. Chem.* **2017**, *65*, 8229–8240.
- (6) Xue, Z.; Li, X.; Li, Y.; Jiang, M.; Liu, H.; Zeng, S.; Hao, J. X-ray-activated near-infrared persistent luminescent probe for deep-tissue and renewable in vivo bioimaging. *ACS Appl. Mater. Inter.* **2017**, *9*, 22132–22142.
- (7) Lv, Y.; Ding, D.; Zhuang, Y.; Feng, Y.; Shi, J.; Zhang, H.; Zhou, T. L.; Chen, H.; Xie, R. J. Chromium-doped zinc gallogermanate@zeolitic imidazolate framework-8: a multifunctional nanoplatfor for rechargeable in vivo persistent luminescence imaging and pH-responsive drug release. *ACS Appl. Mater. Inter.* **2019**, *11*, 1907–1916.
- (8) Li, Y.; Gecevicius, M.; Qiu, J. Long persistent phosphors-from fundamentals to applications. *Chem. Soc. Rev.* **2016**, *45*, 2090–2136.
- (9) Chander, H.; Haranath, D.; Shanker, V.; Sharma, P. Synthesis of nanocrystals of long persisting phosphor by modified combustion technique. *J. Cryst. Growth* **2004**, *271*, 307–312.
- (10) Lecuyer, T.; Teston, E.; Ramirez Garcia, G.; Maldiney, T.; Viana, B.; Seguin, J.; Mignet, N.; Scherman, D.; Richard, C. Chemically engineered persistent luminescence nanoprobes for bioimaging. *Theranostics* **2016**, *6*, 2488–2524.
- (11) Yamamoto, H.; Matsuzawa, T. Mechanism of long phosphorescence of SrAl<sub>2</sub>O<sub>4</sub>:Eu<sup>2+</sup>, Dy<sup>3+</sup> and CaAl<sub>2</sub>O<sub>4</sub>:Eu<sup>2+</sup>, Nd<sup>3+</sup>. *J. Lumin.* **1997**, *72–74*, 287–289.
- (12) Zhuang, Y.; Lv, Y.; Wang, L.; Chen, W.; Zhou, T. L.; Takeda, T.; Hirosaki, N.; Xie, R. J. Trap depth engineering of SrSi<sub>2</sub>O<sub>2</sub>N<sub>2</sub>:Ln<sup>2+</sup>, Ln<sup>3+</sup> (Ln<sup>2+</sup> = Yb, Eu; Ln<sup>3+</sup> = Dy, Ho, Er) persistent luminescence materials for information storage applications. *ACS Appl. Mater. Inter.* **2018**, *10*, 1854–1864.
- (13) Cui, G.; Yang, X.; Zhang, Y.; Fan, Y.; Chen, P.; Cui, H.; Liu, Y.; Shi, X.; Shang, Q.; Tang, B. Round-the-clock photocatalytic hydrogen production with high efficiency by a long-afterglow material. *Angew. Chem. Int. Ed.* **2019**, *58*, 1340–1344.
- (14) Liu, J.; Lecuyer, T.; Seguin, J.; Mignet, N.; Scherman, D.; Viana, B.; Richard, C. Imaging and therapeutic applications of persistent luminescence

- nanomaterials. *Adv. Drug Deliver. Rev.* **2019**, 138, 193–210.
- (15) Luo, Q.; Wang, W.; Tan, J.; Yuan, Q. Surface modified persistent luminescence probes for biosensing and bioimaging: a review. *Chin. J. Chem.* **2021**, 39, 1009–1021.
- (16) Tuerdi, A.; Abd McKayum, A. Dual-functional persistent luminescent nanoparticles with enhanced persistent luminescence and photocatalytic activity. *RSC Adv.* **2019**, 9, 17653–17657.
- (17) Zhao, H. X.; Yang, C. X.; Yan, X. P. Fabrication and bioconjugation of B(III) and Cr(III) co-doped ZnGa<sub>2</sub>O<sub>4</sub> persistent luminescent nanoparticles for dual-targeted cancer bioimaging. *Nanoscale* **2016**, 8, 18987–18994.
- (18) Li, D.; Wang, Y.; Xu, K.; Zhao, H.; Hu, Z. Effect of H<sub>3</sub>BO<sub>3</sub> on the persistent luminescence and photocatalytic properties of ZnGa<sub>2</sub>O<sub>4</sub> phosphors. *Opt. Mater.* **2014**, 36, 1836–1840.
- (19) Abd McKayum, A.; Chen, J. T.; Zhao, Q.; Yan, X. P. Functional near infrared-emitting Cr<sup>3+</sup>/Pr<sup>3+</sup> co-doped zinc gallogermanate persistent luminescent nanoparticles with superlong afterglow for in vivo targeted bioimaging. *J. Am. Chem. Soc.* **2013**, 135, 14125–14133.
- (20) Rosticher, C.; Viana, B.; Fortin, M. A.; Lagueux, J.; Faucher, L.; Chan éac, C. Gadolinium oxysulfide nanoprobe with both persistent luminescent and magnetic properties for multimodal imaging. *RSC Adv.* **2016**, 6, 55472–55478.
- (21) Wang, J.; Ma, Q.; Zheng, W.; Liu, H.; Yin, C.; Wang, F.; Chen, X.; Yuan, Q.; Tan, W. One-dimensional luminous nanorods featuring tunable persistent luminescence for autofluorescence-free biosensing. *ACS Nano* **2017**, 11, 8185–8191.
- (22) Gong, Z.; Liu, Y.; Yang, J.; Yan, D.; Zhu, H.; Liu, C.; Xu, C.; Zhang, H. A Pr<sup>3+</sup> doping strategy for simultaneously optimizing the size and near infrared persistent luminescence of ZGGO:Cr(3+) nanoparticles for potential bio-imaging. *Phys. Chem. Chem. Phys.* **2017**, 19, 24513–24521.
- (23) Li, Y. J.; Yan, X. P. Synthesis of functionalized triple-doped zinc gallogermanate nanoparticles with superlong near-infrared persistent luminescence for long-term orally administrated bioimaging. *Nanoscale* **2016**, 8, 14965–14970.
- (24) Jiang, R.; Yang, J.; Meng, Y.; Yan, D.; Liu, C.; Xu, C.; Liu, Y. X-ray/red-light excited ZGGO:Cr,Nd nanoprobe for NIR-I/II afterglow imaging. *Dalton T.* **2020**, 49, 6074–6083.
- (25) Wang, J.; Ma, Q.; Wang, Y.; Shen, H.; Yuan, Q. Recent progress in biomedical applications of persistent luminescence nanoparticles. *Nanoscale* **2017**, 9, 6204–6218.
- (26) Singh, S. K. Red and near infrared persistent luminescence nano-probes for bioimaging and targeting applications. *RSC Adv.* **2014**, 4, 58674–58698.
- (27) Bessi ère, A.; Jacquart, S.; Priolkar, K.; Lecointre, A.; Viana, B.; Gourier, D. ZnGa<sub>2</sub>O<sub>4</sub>:Cr<sup>3+</sup>: a new red long-lasting phosphor with high brightness. *Opt. Express* **2011**, 19, 10131–10137.
- (28) Allix, M.; Chenu, S.; V éron, E.; Poumeyrol, T.; Kouadri Boudjelthia, E. A.; Alahrach é S.; Porcher, F.; Massiot, D.; Fayon, F. Considerable improvement of long-persistent luminescence in germanium and tin substituted ZnGa<sub>2</sub>O<sub>4</sub>. *Chem. Mater.* **2013**, 25, 1600–1606.
- (29) Dhak, P.; Gayen, U. K.; Mishra, S.; Pramanik, P.; Roy, A. Optical emission spectra of chromium doped nanocrystalline zinc gallate. *J. Appl. Phys.* **2009**, 106, 063721–6.
- (30) Kim, J. S.; Kim, J. S.; Park, H. L. Optical and structural properties of nanosized ZnGa<sub>2</sub>O<sub>4</sub>:Cr<sup>3+</sup> phosphor. *Solid State Commun.* **2004**, 131, 735–738.
- (31) Xu, J.; Murata, D.; Ueda, J.; Viana, B.; Tanabe, S. Toward rechargeable persistent luminescence for the first and third biological windows via persistent energy transfer and electron trap redistribution. *Inorg. Chem.* **2018**, 57, 5194–5203.
- (32) Feng, P.; Li, G.; Guo, H.; Liu, D.; Ye, Q.; Wang, Y. Identifying a cyan ultralong persistent phosphorescence (Ba, Li) (Si, Ge, P)<sub>2</sub>O<sub>5</sub>:Eu<sup>2+</sup>, Pr<sup>3+</sup> via solid solution strategy. *J. Phys. Chem. C* **2019**, 123, 3102–3109.
- (33) Bai, Q.; Zhao, S.; Guan, L.; Wang, Z.; Li, P.; Xu, Z. Design and control of the luminescence of Cr<sup>3+</sup>-doped phosphors in the near-infrared I region by fitting the crystal field. *Cryst. Growth Des.* **2018**, 18, 3178–3186.
- (34) Takahashi, Y.; Ando, M.; Ihara, R.; Fujiwara, T. Green-emissive Mn-activated nanocrystallized glass with willemitte-type Zn<sub>2</sub>GeO<sub>4</sub>. *Opt. Mater. Express* **2011**, 1, 372–378.
- (35) Terraschke, H.; Wickleder, C. UV, blue, green, yellow, red, and small: newest developments on Eu<sup>2+</sup>-doped nanophosphors. *Chem. Rev.* **2015**, 115, 11352–11378.
- (36) Cheng, J.; Li, P.; Wang, Z.; Li, Z.; Tian, M.; Wang, C.; Yang, Z. Color selective manipulation in Li<sub>2</sub>ZnGe<sub>3</sub>O<sub>8</sub>:Mn<sup>2+</sup> by multiple-cation substitution on different crystal-sites. *Dalton T.* **2018**, 47, 4293–4300.
- (37) Li, Z.; Wang, Q.; Wang, Y.; Ma, Q.; Wang, J.; Li, Z.; Li, Y.; Lv, X.; Wei, W.; Chen, L.; Yuan, Q. Background-free latent fingerprint imaging based on nanocrystals with long-lived luminescence and pH-guided recognition. *Nano Res.* **2018**, 11, 6167–6176.
- (38) Feng, Y.; Deng, D.; Zhang, L.; Liu, R.; Lv, Y. LRET-based functional persistent luminescence nanoprobe for imaging and detection of cyanide ion. *Sens. Actuators B-Chem.* **2019**, 279, 189–196.
- (39) Wang, J.; Ma, Q.; Wang, Y.; Li, Z.; Li, Z.; Yuan, Q. New insights into the structure-performance relationships of mesoporous materials in analytical science. *Chem. Soc. Rev.* **2018**, 47, 8766–8803.
- (40) Liu, H.; Hu, X.; Wang, J.; Liu, M.; Wei, W.; Yuan, Q. Direct low-temperature synthesis of ultralong persistent luminescence nanobelts based on a biphasic solution-chemical reaction. *Chin. Chem. Lett.* **2018**, 29, 1641–1644.
- (41) Wang, Y.; Wang, J.; Ma, Q.; Li, Z.; Yuan, Q. Recent progress in background-free latent fingerprint imaging. *Nano Res.* **2018**, 11, 5499–5518.
- (42) Cheng, S.; Shen, B.; Yuan, W.; Zhou, X.; Liu, Q.; Kong, M.; Shi, Y.; Yang, P.; Feng, W.; Li, F. Time-gated ratiometric detection with the same

- working wavelength to minimize the interferences from photon attenuation for accurate in vivo detection. *ACS Cent. Sci.* **2019**, *5*, 299–307.
- (43) Ou, X. Y.; Guo, T.; Song, L.; Liang, H. Y.; Zhang, Q. Z.; Liao, J. Q.; Li, J. Y.; Li, J.; Yang, H. H. Autofluorescence-free immunoassay using X-ray scintillating nanotags. *Anal. Chem.* **2018**, *90*, 6992–6997.
- (44) Wang, J.; Ma, Q.; Liu, H.; Wang, Y.; Shen, H.; Hu, X.; Ma, C.; Yuan, Q.; Tan, W. Time-gated imaging of latent fingerprints and specific visualization of protein secretions via molecular recognition. *Anal. Chem.* **2017**, *89*, 12764–12770.
- (45) Shen, H.; Wang, Y.; Wang, J.; Li, Z.; Yuan, Q. Emerging biomimetic applications of DNA nanotechnology. *ACS Appl. Mater. Inter.* **2019**, *11*, 13859–13873.
- (46) Jia, D.; Jia, W.; Evans, D. R.; Dennis, W. M.; Liu, H.; Zhu, J.; Yen, W. M. Trapping processes in  $\text{CaS:Eu}^{2+}, \text{Tm}^{3+}$ . *J. Appl. Phys.* **2000**, *88*, 3402–3407.
- (47) Guo, C.; Tang, Q.; Huang, D.; Zhang, C.; Su, Q. Tunable color emission and afterglow in  $\text{CaGa}_2\text{S}_4:\text{Eu}^{2+}, \text{Ho}^{3+}$  phosphor. *Mater. Res. Bull.* **2007**, *42*, 2032–2039.
- (48) Denis, G.; Deniard, P.; Rocquefelte, X.; Benabdesselam, M.; Jobic, S. The thermally connected traps model applied to the thermoluminescence of  $\text{Eu}^{2+}$  doped  $\text{Ba}_{13-x}\text{Al}_{22-2x}\text{Si}_{10+2x}\text{O}_{66}$  materials ( $x \sim 0.6$ ). *Opt. Mater.* **2010**, *32*, 941–945.
- (49) Struve, B.; Huber, G. The effect of the crystal field strength on the optical spectra of  $\text{Cr}^{3+}$  in gallium garnet laser crystals. *Appl. Phys. B* **1985**, *36*, 195–201.
- (50) Forster, L. S. The photophysics of chromium(III) complexes. *Chem. Rev.* **1990**, *90*, 331–353.
- (51) Maldiney, T.; Lecointre, A.; Viana, B.; Bessiere, A.; Bessodes, M.; Gourier, D.; Richard, C.; Scherman, D. Controlling electron trap depth to enhance optical properties of persistent luminescence nanoparticles for in vivo imaging. *J. Am. Chem. Soc.* **2011**, *133*, 11810–11815.
- (52) Jia, G.; Lewis, L.; Wang, X.  $\text{Cr}^{3+}$ -doped lanthanum gallogermanate phosphors with long persistent IR emission. *Electrochem. Solid St.* **2010**, *13*, J32–J34.
- (53) Aitasalo, T.; Dereñ, P.; Hölsä, J.; Jungner, H.; Krupa, J. C.; Lastusaari, M.; Legendziewicz, J.; Niittykoski, J.; Stręk, W. Persistent luminescence phenomena in materials doped with rare earth ions. *J. Solid State Chem.* **2003**, *171*, 114–122.
- (54) Li, X.; Zhang, F.; Zhao, D. Highly efficient lanthanide upconverting nanomaterials: progresses and challenges. *Nano Today* **2013**, *8*, 643–676.
- (55) Dong, H.; Sun, L. D.; Yan, C. H. Basic understanding of the lanthanide related upconversion emissions. *Nanoscale* **2013**, *5*, 5703–5714.
- (56) Cai, Y.; Liu, B.; Chen, W.; Qiu, J.; Xu, X.; Zhao, L.; Yu, X. X-ray and UV excited long persistent luminescence properties of  $\text{Zn}_3\text{Ga}_2\text{GeO}_8: \text{Cr}^{3+}, \text{Pr}^{3+}$ . *ECS J. Solid State Sc.* **2020**, *9*, 066006–7.
- (57) Sun, S. K.; Wang, H. F.; Yan, X. P. Engineering persistent luminescence nanoparticles for biological applications: from biosensing/bioimaging to theranostics. *Acc. Chem. Res.* **2018**, *51*, 1131–1143.
- (58) Qu, B.; Zhang, B.; Wang, L.; Zhou, R.; Zeng, X. C. Mechanistic study of the persistent luminescence of  $\text{CaAl}_2\text{O}_4:\text{Eu}, \text{Nd}$ . *Chem. Mater.* **2015**, *27*, 2195–2202.
- (59) Pan, Z.; Lu, Y. Y.; Liu, F. Sunlight-activated long-persistent luminescence in the near-infrared from  $\text{Cr}^{3+}$ -doped zinc gallogermanates. *Nat. Mater.* **2011**, *11*, 58–63.
- (60) Wang, F.; Han, Y.; Lim, C. S.; Lu, Y.; Wang, J.; Xu, J.; Chen, H.; Zhang, C.; Hong, M.; Liu, X. Simultaneous phase and size control of upconversion nanocrystals through lanthanide doping. *Nature* **2010**, *463*, 1061–1065.
- (61) Mikami, M.; Oshiyama, A. First-principles study of intrinsic defects in yttrium oxysulfide. *Phys. Rev. B* **1999**, *60*, 1707–1715.
- (62) Li, P.; Peng, M.; Wondraczek, L.; Zhao, Y.; Viana, B. Red to near infrared ultralong lasting luminescence from  $\text{Mn}^{2+}$ -doped sodium gallium aluminum germanate glasses and (Al,Ga)-albite glass-ceramics. *J. Mater. Chem. C* **2015**, *3*, 3406–3415.
- (63) Kandpal, S. K.; Goundie, B.; Wright, J.; Pollock, R. A.; Mason, M. D.; Meulenbergh, R. W. Investigation of the emission mechanism in milled  $\text{SrAl}_2\text{O}_4:\text{Eu}, \text{Dy}$  using optical and synchrotron X-ray spectroscopy. *ACS Appl. Mater. Inter.* **2011**, *3*, 3482–3486.
- (64) Liu, J. M.; Liu, Y. Y.; Zhang, D. D.; Fang, G. Z.; Wang, S. Synthesis of  $\text{GdAlO}_3:\text{Mn}^{4+}, \text{Ge}^{4+}@\text{Au}$  core-shell nanoprobes with plasmon-enhanced near-infrared persistent luminescence for in vivo trimodality bioimaging. *ACS Appl. Mater. Inter.* **2016**, *8*, 29939–29949.
- (65) Li, Y.; Li, Y. Y.; Sharafudeen, K.; Dong, G. P.; Zhou, S. F.; Ma, Z. J.; Peng, M. Y.; Qiu, J. R. A strategy for developing near infrared long-persistent phosphors: taking  $\text{MAlO}_3:\text{Mn}^{4+}, \text{Ge}^{4+}$  ( $M = \text{La}, \text{Gd}$ ) as an example. *J. Mater. Chem. C* **2014**, *2*, 2019–2027.
- (66) Rosticher, C.; Viana, B.; Laurent, G.; Le Griel, P.; Chan'ac, C. Insight into  $\text{CaMgSi}_2\text{O}_6:\text{Eu}^{2+}, \text{Mn}^{2+}, \text{Dy}^{3+}$  nanoprobes: influence of chemical composition and crystallinity on persistent red luminescence. *Eur. J. Inorg. Chem.* **2015**, 3681–3687.
- (67) Katayama, Y.; Hashimoto, A.; Xu, J.; Ueda, J.; Tanabe, S. Thermoluminescence investigation on  $\text{Y}_3\text{Al}_{5-x}\text{Ga}_x\text{O}_{12}:\text{Ce}^{3+}, \text{Bi}^{3+}$  green persistent phosphors. *J. Lumin.* **2017**, *183*, 355–359.
- (68) Zhuang, Y.; Katayama, Y.; Ueda, J.; Tanabe, S. A brief review on red to near-infrared persistent luminescence in transition-metal-activated phosphors. *Opt. Mater.* **2014**, *36*, 1907–1912.
- (69) Ueda, J.; Aishima, K.; Nishiura, S.; Tanabe, S. Afterglow luminescence in  $\text{Ce}^{3+}$ -doped  $\text{Y}_3\text{Sc}_2\text{Ga}_3\text{O}_{12}$  ceramics. *Appl. Phys. Express* **2011**, *4*, 042602–3.
- (70) Li, K.; Shang, M.; Zhang, Y.; Fan, J.; Lian, H.; Lin, J. Photoluminescence properties of single-component white-emitting  $\text{Ca}_9\text{Bi}(\text{PO}_4)_7:\text{Ce}^{3+}, \text{Tb}^{3+}, \text{Mn}^{2+}$  phosphors for UV LEDs. *J. Mater. Chem. C* **2015**, *3*, 7096–7104.
- (71) Zeng, W.; Wang, Y.; Han, S.; Chen, W.; Li, G.; Wang, Y.; Wen, Y. Design, synthesis and characterization of a novel yellow long-persistent phosphor:

Ca<sub>2</sub>BO<sub>3</sub>Cl:Eu<sup>2+</sup>,Dy<sup>3+</sup>. *J. Mater. Chem. C* **2013**, 1, 3004–3011.

- (72) Trojan Piegza, J.; Niittykoski, J.; Häsä J.; Zych, E. Thermoluminescence and kinetics of persistent luminescence of vacuum-sintered Tb<sup>3+</sup>-doped and Tb<sup>3+</sup>,Ca<sup>2+</sup>-codoped Lu<sub>2</sub>O<sub>3</sub> materials. *Chem. Mater.* **2008**, 20, 2252–2261.
- (73) Cao, C.; Guo, S.; Moon, B. K.; Choi, B. C.; Jeong, J. H. Synthesis, grouping, and optical properties of RE<sub>F3</sub>-KF nanocrystals. *Mater. Chem. Phys.* **2013**, 139, 609–615.
- (74) Zhang, H.; Zheng, M.; Lei, B.; Liu, Y.; Xiao, Y.; Dong, H.; Zhang, Y.; Ye, S. Luminescence properties of red long-lasting phosphorescence phosphor AlN:Mn<sup>2+</sup>. *ECS J. Solid State Sci. Technol.* **2013**, 2, R117–R120.

## Influence of Doped Ions on Persistent Luminescence Materials: a Review

ZHANG Liu-Wei(张留伟) SHEN Rui-Chen(沈瑞晨) TAN Jie(谈洁) YUAN Quan(袁荃)

Doped ions will directly affect the luminescence centers and trap levels of persistent luminescence materials (PLMs), thereby leading to great differences in the optical performance. Herein, we discuss how doped ions affect the structure and optical performance of PLMs based on the types of doped ions, the number of the types of doped ions and the content of doped ions.

